BIG BROTHER Uncouples Cell Proliferation from Elongation in the Arabidopsis Primary Root

Pietro Cattaneo and Christian S. Hardtke*

Department of Plant Molecular Biology, University of Lausanne, Biophore Building, CH-1015 Lausanne, Switzerland
*Corresponding author: E-mail, christian.hardtke@unil.ch; Fax, +41-21-692-4150.

Plant organ size is sensitive to environmental conditions, but is also limited by hardwired genetic constraints. In Arabidopsis, a few organ size regulators have been identified. Among them, the _BIG BROTHER_ (_BB_) gene has a prominent role in the determination of flower organ and leaf size. _BB_ loss-of-function mutations result in a prolonged proliferation phase during leaf(-like) organ formation, and consequently larger leaves, petals and sepals. Whether _BB_ has a similar role in root growth is unknown. Here we describe a novel _bb_ allele which carries a P235L point mutation in the BB RING finger domain. This allele behaves similarly to described _bb_ loss-of-function alleles and displays increased root meristem size due to a higher number of dividing, meristematic cells. In contrast, mature cell length is unaffected. The increased meristematic activity does not, however, translate into overall enhanced root elongation, possibly because _bb_ mutation also results in an increased number of cell files in the vascular cylinder. These extra formative divisions might offset any growth acceleration by extra meristematic divisions. Thus, although _BB_ dampens root cell proliferation, the consequences on macroscopic root growth are minor. However, _bb_ mutation accelerates overall root growth when introduced into sensitized backgrounds. For example, it partially rescues the short root phenotypes of the _brevis radix_ and _octopus_ mutants, but does not complement their phloem differentiation or transport defects. In summary, we provide evidence that _BB_ acts conceptually similarly in leaf(-like) organs and the primary root, and uncouples cell proliferation from elongation in the root meristem.

Introduction

Plant organ size can vary as a function of environmental conditions; however, this variation operates within the limits set by genetic constraints. The underlying genetic factors can be revealed in standardized growth conditions that even out plant ontogeny. Moreover, they are most evident in structures whose size shows comparatively little variation in response to the environment, such as seeds or flower organs of the model plant _Arabidopsis thaliana_ (Arabidopsis). Through a forward genetic screen, the _BIG BROTHER_ (_BB_) gene of Arabidopsis has been identified as a negative regulator of petal size (Disch et al. 2006). _BB_ loss-of-function mutations result in bigger petals, and _BB_ gain of function, through ectopic overexpression, induces the opposite phenotype (Disch et al. 2006, Vanhaeren et al. 2017). In the loss-of-function scenario, final cell size is not affected, while in the gain-of-function scenario, a slight, possibly compensatory cell size increase could be observed. Nevertheless, a priori the organ size variation can be explained by differences in cell number. For instance, in _bb_ loss-of-function mutants, cell number is increased. However, this is not due to an accelerated cell cycle, but rather due to a delay in the transition from proliferation to elongation (Disch et al. 2006, Li et al. 2008, Vanhaeren et al. 2017).

_BB_ encodes an E3 ubiquitin ligase with a RING finger domain that is essential for its activity (Disch et al. 2006). Another RING finger-type E3 ligase, DA2, plays a similar role to BB in organ size determination (Xia et al. 2013). _bb_ and _da2_ mutants enhance each other's phenotype in an additive manner, suggesting that the two genes work genetically independently of each other. They also enhance the phenotype of another, dominant-negative mutant with increased organ size due to a prolonged cell proliferation phase, _da1-1_ (Li et al. 2008, Xia et al. 2013, Du et al. 2014, Vanhaeren et al. 2017). A recent study has demonstrated that both BB and DA2 ubiquitinate DA1, a peptidase with ubiquitin interaction motifs (UIMs), which thereby becomes activated (Dong et al. 2017). Although this apparently destabilizes BB and DA2 in turn, DA1 might be required for efficient target recognition and/or degradation by BB and DA2, which would explain the similar phenotypes of the three loss-of-function mutants and their mutual enhancement (Dong et al. 2017).

_DA1_ acts partially redundantly with one of its homologs, _DA1-RELATED 1_ (_DAR1_) (Li et al. 2008, Dong et al. 2017). Interestingly, loss of function in another homolog, _DAR2_, has been reported to affect root meristem activity, however in an opposite sense, as would be expected from the _da1/dar1_ precedence (Peng et al. 2013). _dar2_ mutants display reduced cell proliferation in the root meristem and increased mature cell length which, however, do not compensate each other and lead

to substantially reduced root growth (Peng et al. 2013). Thus, *DAR2* mutation appears to accelerate the transition from root cell proliferation to differentiation–elongation. However, unlike DA1 or DAR1, DAR2 does not contain UIMs (Peng et al. 2013), and therefore its biochemical function might be distinct. Whether *da1*, *bb* or *dar1* mutants display root phenotypes has not been reported; however, *BB* is expressed in the root (Disch et al. 2006). Here we demonstrate that *BB* has a conceptually similar role in the root and in the shoot. *bb* mutants display increased root meristem size in terms of cell number, in both the longitudinal and radial dimensions. Although the impact of this phenotype on overall, macroscopic root growth is minor, it gains in importance in sensitized backgrounds.

Results

Arabidopsis mutants in the *BREVIS RADIX* (*BRX*) gene display a short root phenotype (Mouchel et al. 2004), which is the consequence of impaired protophloem development in the root meristem of *brx* mutants (Rodriguez-Villalon et al. 2014). The occurrence of sieve element precursors that do not undergo differentiation presumably leads to interrupted sieve tubes in *brx* mutants and is associated with a number of systemic effects, such as reduced auxin activity throughout the root meristem and increased lateral root branching (Mouchel et al. 2006, Gujas et al. 2012, Rodriguez-Villalon et al. 2015). At the morphological level, the *brx* short root phenotype can be explained by a combination of strongly reduced meristematic activity and lightly reduced cell elongation (Mouchel et al. 2004). In an attempt to isolate second site genetic modifiers of this phenotype, we have conducted a suppressor screen for mutants which fully or partially restore *brx* root growth vigor (Depuydt et al. 2013, Rodriguez-Villalon et al. 2014, Rodriguez-Villalon et al. 2015, Kang and Hardtke 2016). One of the lines isolated displayed an intermediate phenotype of partial yet substantial suppression of impaired *brx* root growth. Genetic mapping by whole-genome sequencing of bulked segregants (Depuydt et al. 2013) pointed to a mutation in the *BB* gene (At3g63530) as probably causative. This C to T change gives rise to an amino acid substitution, P235L, directly C-terminal to the penultimate cysteine of the BB RING finger domain (**Fig. 1A**).

To verify independently whether BB mutation could indeed be responsible for the second site suppression, we obtained the *bb-2* allele, which is in the same Columbia-0 (Col-0) background and carries a T-DNA insertion in the *BB* 5′ region that leads to a strong down-regulation of *BB* expression (Disch et al. 2006). In the F$_2$ of crosses to the *brx* mutant, the segregation of short root vs. intermediate root length individuals suggested that *bb-2* can suppress the *brx* phenotype (Supplementary Fig. S1A), which was eventually confirmed in subsequently isolated *bb-2 brx* double mutants (**Fig. 1B, C**). Therefore, although the residue corresponding to P235 in BB is typically not conserved across RING finger domains (Kosarev et al. 2002), it is apparently important for BB activity, because the P235L mutation leads to a loss of function. In summary, our data show that *bb*
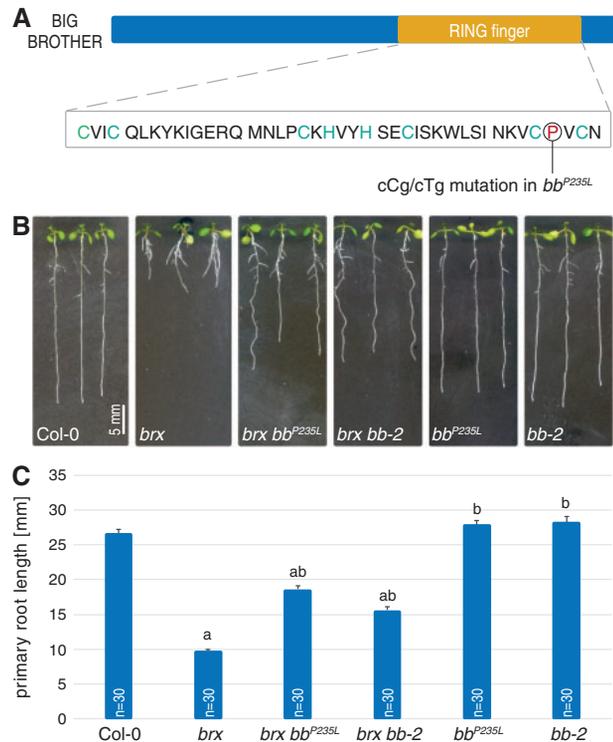
Fig. 1 Second site mutation in *BB* partially suppresses reduced *brx* root growth. (A) Schematic presentation of the BB protein, and the position and sequence of the RING finger domain, highlighting the mutation leading to the P235L amino acid change. (B) Representative seedlings of the indicated genotypes, at 7 d after germination (dag). (C) Average primary root length of the indicated genotypes, at 7 dag. Differences as compared with the Col-0 wild-type background (a) or *brx* mutant background (b) are statistically significant as indicated (Student's *t*-test; *P* < 0.001; mean ± SEM).

loss-of-function mutations are second site suppressors of the *brx* root phenotype.

To determine whether *brx* suppression by *bb* reflects a role for *BB* in phloem development, we analyzed *bb brx* double mutants in further detail. A key feature of *brx* mutants is the occurrence of non-differentiated, so-called gap cells in the protophloem transition zone (Rodriguez-Villalon et al. 2014) (**Fig. 2A**). Perfect *brx* suppressors, such as loss of function in *BARELY ANY MERISTEM 3* (*BAM3*) (Depuydt et al. 2013), do not only fully rescue the short root phenotype, but also fully restore proper sieve element differentiation. In *bb brx* double mutants, this was not the case (**Fig. 2B**). Consistently, impaired phloem sap delivery to the root meristem (a consequence of the gap cells) was not rescued either, as illustrated by the strongly reduced phloem-mediated translocation of carboxyfluorescein diacetate (CFDA) dye from the cotyledons to the root phloem unloading zone (**Fig. 2C–E**). Moreover, *bb brx* as well as *bb* mutants were fully sensitive to the BAM3 ligand CLAVATA3/ EMBRYO SURROUNDING REGION 45 (CLE45) (**Fig. 2F**). Thus, *BB* apparently does not affect CLE45 perception, which negatively regulates protophloem formation through BAM3 (Depuydt et al. 2013). Also, auxin activity, as judged from the abundance of the DII-VENUS reporter (Santuari et al. 2011), was
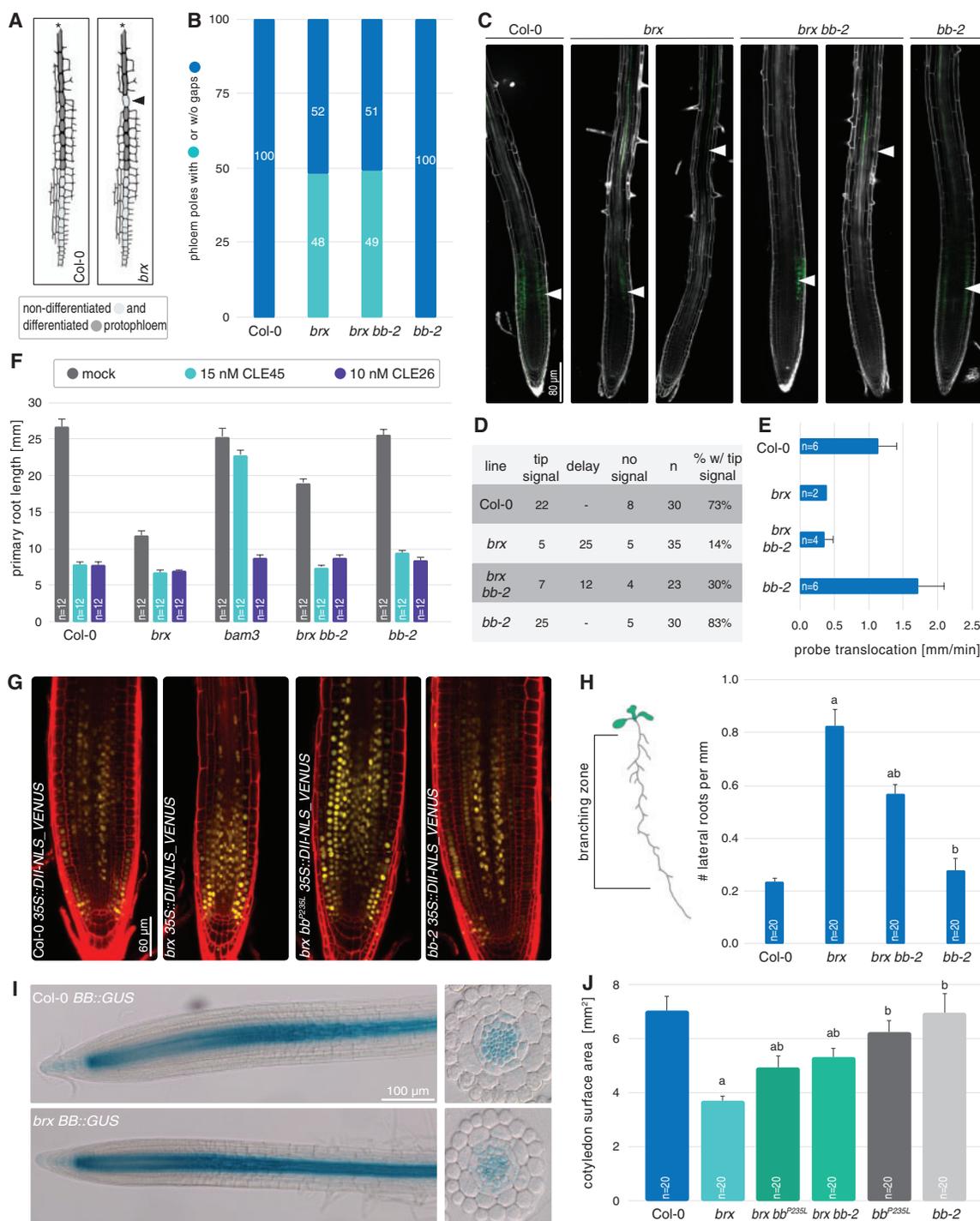
Fig. 2 Evaluation of local and systemic phenotypes in *bb brx* double mutant roots. (A) Schematic overview of developing protophloem sieve element strands, highlighting the occurrence of undifferentiated 'gap' cells (arrowhead) in *brx* mutants. (B) Quantification of gap cell frequency in the indicated genotypes at 7 d after germination (dag). Differences between Col-0 and *bb-2* vs. *brx* and *bb-2 brx* were statistically significant (*P* < 0.001, Fisher's exact test), but not within those pairs. (C) Phloem-mediated translocation of CFDA dye (green fluorescence, arrowheads) into the phloem unloading zone of the root tip, 45 min after CFDA application to the cotyledons of 4-day-old seedlings. Representative seedlings for the indicated phenotypes [white fluorescence: propidium iodide (PI) cell wall staining] are shown. (D) Corresponding classification of the CFDA signal at the end of the experiment. (E) CFDA translocation velocity in vivo measurements, based exclusively on seedlings in which it reached the root tip. (F) Primary root growth response of the indicated genotypes to the presence of CLE peptides in the medium at 7 dag. All treatments were statistically significant as compared with mock treatment (*P* < 0.001, Student's *t*-test), except for *bam3* on CLE45. (G) Auxin activity in the indicated genotypes at 7 dag as monitored by the DII-VENUS inverse reporter (yellow fluorescence), composite images (red fluorescence: PI staining). (H) Lateral root density in the indicated genotypes at 12 dag. (I) GUS reporter staining of *BB* expression in the indicated genotypes at 7 dag. (J) Cotyledon surface area in the indicated genotypes at 9 dag. Differences as compared with the Col-0 wild-type background (a) or *brx* mutant background (b) are statistically significant as indicated (Student's *t*-test; *P* < 0.01; mean ± SEM).

not markedly increased in *bb brx* mutants as compared with *brx* single mutants (**Fig. 2G**). However, we noticed a slight reduction in lateral root density (**Fig. 2H**), which could also reflect the observation that mature cell length was partially rescued (see below). Finally, we confirmed that *BB* is expressed in the root, in the vascular cylinder (Disch et al. 2006). We also verified that *bb* loss of function does not suppress *brx* because of an effect of *BRX* loss of function on *BB* expression, i.e. *BB* is not overexpressed in a *brx* background (**Fig. 2I**).

In summary, although *bb* mutation substantially rescued the reduced root growth of *brx*, this does not appear to be due to a specific *BB* function in protophloem development, but rather to a generic effect on root growth. In support of this, we also observed rescue of the reduced cotyledon size of *brx* (Beuchat et al. 2010) (**Fig. 2J**), and restoration of *brx* root meristem size to nearly wild-type levels, as indicated by the number of meristematic cortex cells (**Fig. 3A, B**). To verify whether *bb* mutation already has an effect on root growth by itself, we investigated the *bb-2* mutant as well as the *bb*[P235L] mutant (recovered from crosses of the suppressor line to Col-0) in more detail. Neither of the two alleles displayed any significant difference from the wild type in terms of root growth vigor (**Fig. 1C**). This was also true when *bb* root growth was monitored on other, suboptimal growth media (e.g. without sucrose) (Supplementary Fig. S1B). However, surprisingly, in both mutants the meristems were clearly larger than in the wild type (**Fig. 3A, B**). Nevertheless, an impact on root growth could also not be detected over an extended time period (**Fig. 3C**). The larger *bb* meristem was also obvious in the cumulative cortex cell lengths along the meristem (**Fig. 3D**), which allowed us to calculate the switching point between cell proliferation and the transition to differentiation–elongation (Supplementary Fig. S1C). This switch point was consistently later in *bb* than in the wild type (**Fig. 3E**). However, the apparently prolonged cell proliferation phase had no marked effect on cell size, because the length of both proliferating and mature cortex cells was similar in *bb* and Col-0 (**Fig. 3F, G**). Thus, *bb* mutation apparently permits a longer phase of cell proliferation before cell expansion in the root meristem, similar to its role in the shoot. While these observations suggest that despite their larger meristem, *bb* roots do not grow overall faster than those of the wild type, the effects of *BB* loss of function apparently manifest in sensitized backgrounds such as *brx*. Consistent with the partially rescued *brx* root growth, *bb* second site mutation not only normalized root meristem size, but also recovered the switch point, as well as, in part, mature cell length (**Fig. 3B–G**).

Potential discrepancies between meristem size, mature cell length and overall root growth vigor can sometimes be explained by altered frequency of formative divisions, which give rise to root cell files. For example, the short root phenotype of brassinosteroid receptor mutants can be explained quantitatively by a combination of reduced mature cell size and a slowing down of root growth by supernumerary formative cell divisions (Kang et al. 2017). Indeed, cross-sections of *bb* mutants revealed a marked increase in cell file number in the *BB* expression domain, i.e. the endodermis, the pericycle and the vascular cylinder (**Fig. 4A, B**). Thus, cell number was not markedly increased in the longitudinal, but also in the radial dimension of *bb* root meristems. Notably, the supernumerary formative divisions did not impinge on vascular tissue organization. Moreover, they did not substantially increase the vascular cylinder area (**Fig. 4C**), but rather resulted in smaller cells (in the radial dimension) and therefore presumably more anisotropic cells (**Fig. 4D**). This effect was also observed in the respective *bb brx* double mutants, again indicating that *BB* acts independently of *BRX* in root development.

To verify this notion in an independent scenario, we also crossed the *bb-2* mutant to a loss-of-function allele of *OCTOPUS* (*OPS*), another positive regulator of protophloem development (Truernit et al. 2012, Rodriguez-Villalon et al. 2014). The *brx* and *ops* mutant root phenotypes are essentially identical, including the systemic effects (Truernit et al. 2012, Rodriguez-Villalon et al. 2014, Rodriguez-Villalon et al. 2015, Kang et al. 2017). Similar to *bb brx* double mutants, the reduced root growth of *ops* mutants was partially compensated by *bb* second site mutation (**Fig. 5A, B**). However, again the more specific defects of *ops* were not complemented (**Fig. 5C–E**), while cell number was increased in both the longitudinal and radial dimensions (**Fig. 5F, G**). Therefore, *BB* also appears to act independently of *OPS* in root development, corroborating its generic role as a growth repressor.

Discussion

Within the limits of constraints dictated by environmental factors, plant organ size is genetically determined (Breuninger and Lenhard 2010, Gonzalez and Inze 2015). This is most conspicuous in organs whose size is comparatively invariable, such as petals. The *BB* gene was indeed originally identified because of the effect of its loss of function on petal size, but it soon became clear that it also affected the size of other leaf(-like) organs (Disch et al. 2006, Li et al. 2008). Kinetic analyses of leaf development suggest that this phenotype is due to a role for *BB* in limiting the cell proliferation phase, and promoting the transition to differentiation and cell expansion (Disch et al. 2006, Li et al. 2008, Vanhaeren et al. 2017). This appears to be a general theme in organ size determination, since a similar role has been described for other pertinent factors (Krizek, 1999, Mizukami and Fischer 2000, Hu et al. 2003), which presumably act in parallel to the BB–DA1–DA2 network (Disch et al. 2006, Dong et al. 2017). Here we found that *BB* has a conceptually similar role in the determination of primary root meristem size. *bb* loss-of-function alleles display increased meristematic cell number, but no alteration in mature cell length. This phenotype is remarkable, given reports that a shift in the relative size of the root meristem's proliferation or differentiation–elongation zones is typically associated with altered mature cell length (Moubayidin et al. 2010, Scacchi et al. 2010, Depuydt and Hardtke 2011, Perilli et al. 2012, Peng et al. 2013, Mahonen et al. 2014). The phenotype of *bb* mutants is therefore more similar to that obtained by ectopic overexpression of PLETHORA (PLT) transcription factors, which promote the expression of cell proliferation genes, but suppress the expression
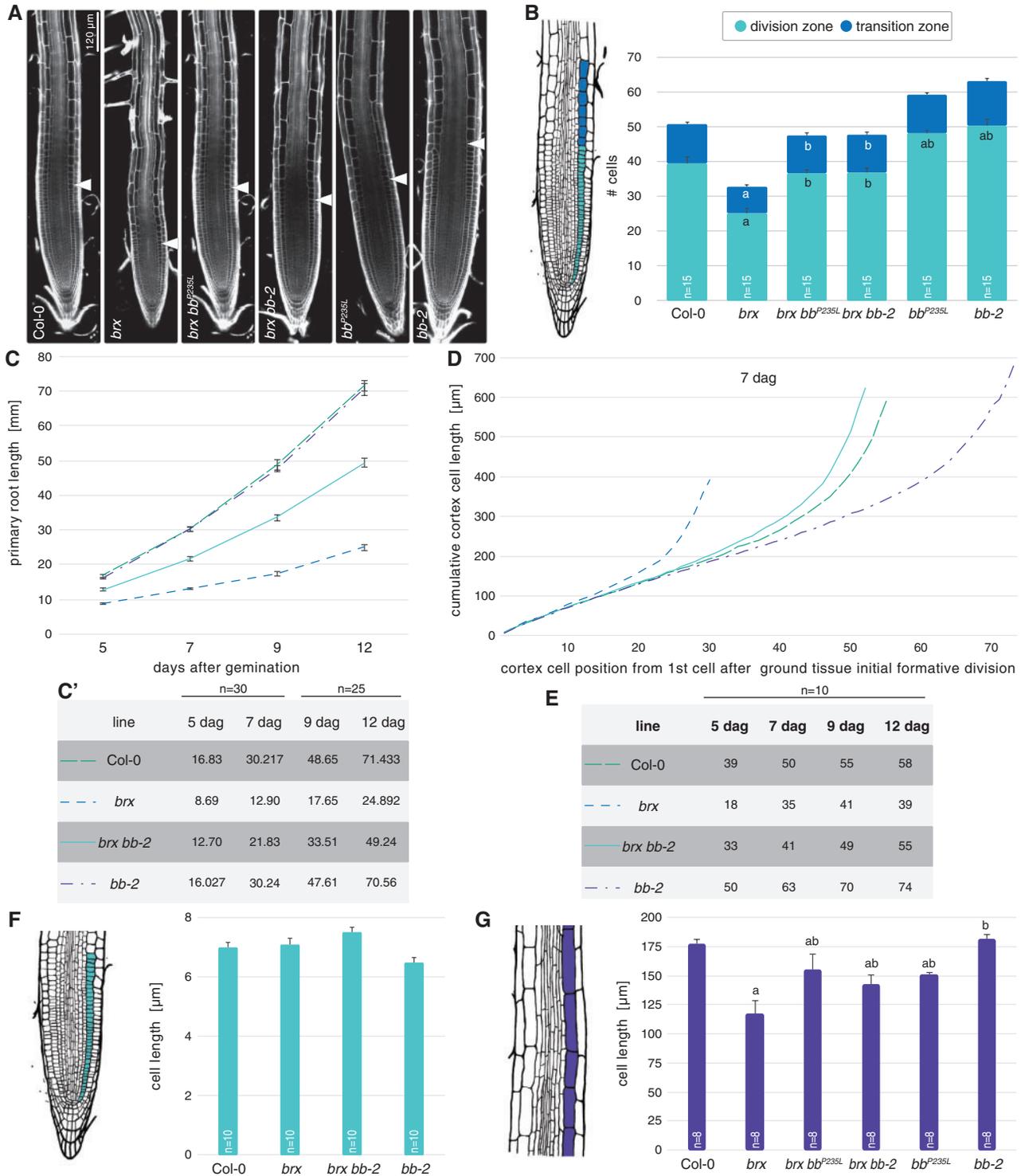
Fig. 3 Cell proliferation in *bb* root meristems. (A) Representative root meristems of the indicated genotypes at 7 d after germination (dag), confocal microscopy [white fluorescence: propidium iodide (PI) staining]. Arrowheads indicate the approximate location of the proliferation to differentiation–elongation switch. (B) Quantification of cortex cell number in the division zone and transition zone of 7-day-old seedlings of the indicated genotypes. (C) Root growth progression in the indicated phenotypes over time. Differences between *brx* and *brx bb-2*, and between those two genotypes and Col-0 and *bb-2* were statistically significant (*P* < 0.001; Student's *t*-test) at every time point (C′: data for individual time points). (D) Progression of cortex cell elongation along the meristems of 7-day-old roots of the indicated genotypes. (E) Calculations for the switch between proliferation and transition in cortex cell files of the indicated genotypes, with respect to the first cell after the formative ground tissue division. (F) Length of proliferating cortex cells in the indicated genotypes at 7 dag. Average of the average for 10 roots, with 20–45 cells scored per root. (G) Length of mature cortex cells in the indicated genotypes at 7 dag. Average of the average for eight roots, with approximately 10 cells scored per root. Differences as compared with the Col-0 wild-type background (a) or *brx* mutant background (b) are statistically significant as indicated (Student's *t*-test; *P* < 0.05; mean ± SEM).
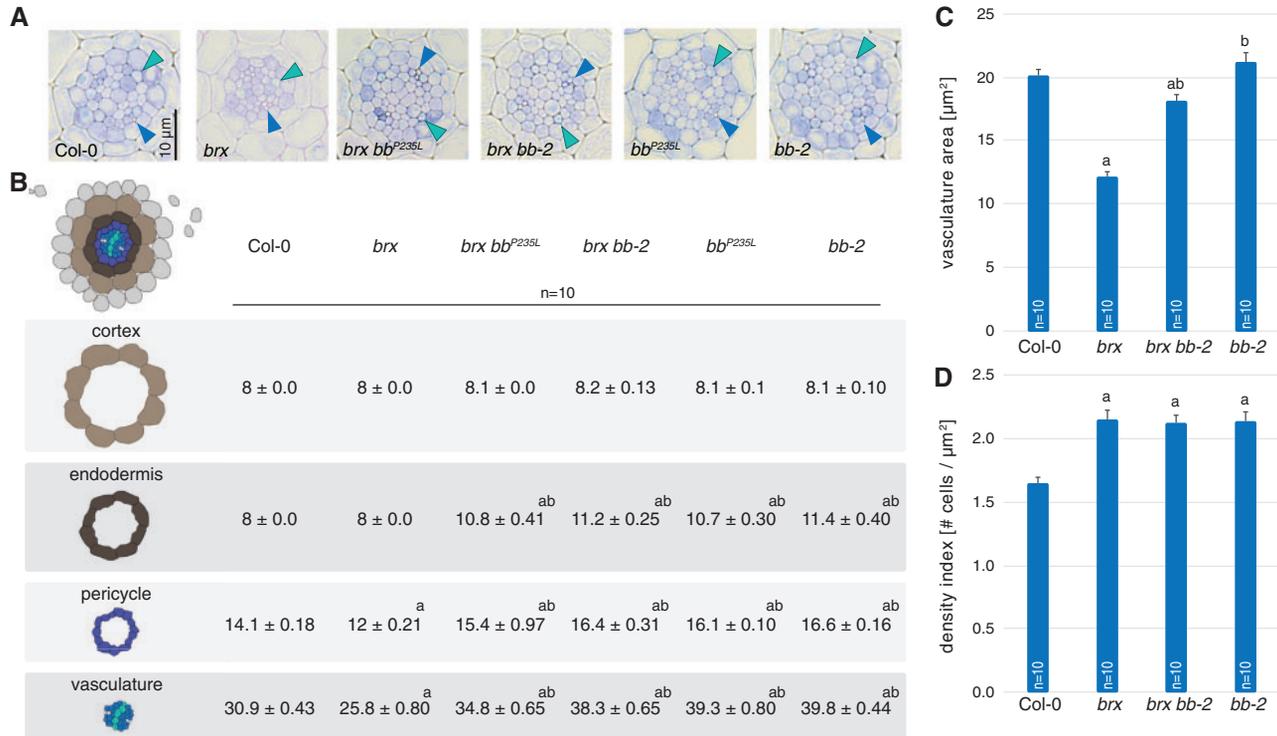
Fig. 4 Formative divisions in *bb* root meristems. (A) Representative histological cross-sections of 6-day-old roots of the indicated genotypes, taken at the position where protoxylem (green arrowheads) has differentiated (blue arrowheads: protophloem). (B) Quantification of cell file number in roots of the indicated genotypes at 6 d after germination (dag). (C) Quantification of vascular cylinder area in roots of the indicated genotypes at 6 dag. (D) Quantification of cell file density in the vascular cylinder in roots of the indicated genotypes at 6 dag. Differences as compared with the Col-0 wild-type background (a) or *brx* mutant background (b) are statistically significant as indicated (Student's *t*-test; $P < 0.01$; mean ± SEM).

of genes involved in differentiation (Mahonen et al. 2014, Santuari et al. 2016). However, whether *PLT* gain of function also affects mature cell size has not been reported in detail. In summary, our results suggest that *bb* mutation prolongs the cell proliferation phase in the root meristem, but does not affect mature cell length, thereby uncoupling root meristematic activity from cell elongation. Because this effect is observed in the cortex cell layer, where *BB* does not appear to be expressed, it also suggests co-ordination of growth between layers through non-cell-autonomous signals, as previously observed (Kang et al. 2017).

Surprisingly, the increased cell proliferation in *bb* meristems did not translate into enhanced overall root growth in our standard conditions, with a limit of observation at 12 d after germination. Therefore, within the limits of our experimental set-up, *BB* mutation had no macroscopic effect on root growth. On the one hand, this might in part be explained by the increased number of formative cell divisions in the stele, which could lead to a temporal slowing down of root growth as observed in other, similar scenarios (De Rybel et al. 2013, Kang et al. 2017). On the other hand, unchanged overall root growth and mature cell size suggest an unchanged overall output of differentiated cells by the *bb* meristem. This in turn implies that the division rate of each individual cell might be reduced (Beemster and Baskin 1998, Beemster et al. 2002). However, a stimulatory effect of *bb*

second site mutation was observed in the *brx* and *ops* backgrounds, in which root growth is strongly reduced because of impaired protophloem differentiation (Truernit et al. 2012, Rodriguez-Villalon et al. 2014, Rodriguez-Villalon et al. 2015). Notably, the partial rescue of *brx* or *ops* by *bb* was not associated with a marked restoration of reported systemic defects, such as reduced auxin activity or phloem sap delivery. This is consistent with the persistence of the protophloem differentiation defects in *bb brx* or *bb ops* double mutants. The only exception was the reduced density of lateral roots, which scaled with the rescue of primary root growth however, and could also be simply explained by the partially rescued mature cell length. Thus, *bb* mutation can influence cell elongation; however, it appears that this only becomes evident in genetic backgrounds in which the cell proliferation phase is severely shortened and cell differentiation is accelerated (Mouchel et al. 2004, Truernit et al. 2012). Moreover, the slightly reduced number of formative divisions in the *brx* and *ops* vascular cylinders (Rodriguez-Villalon et al. 2015) was overcompensated by *bb* second site mutation, corroborating that *BB* appears to act locally and largely independently of systemic inputs. In line with this notion, *BB* was for instance not found among the PLT target genes (Santuari et al. 2016).

In summary, we demonstrate that *bb* loss-of-function mutations prolong the cell proliferation phase in the root
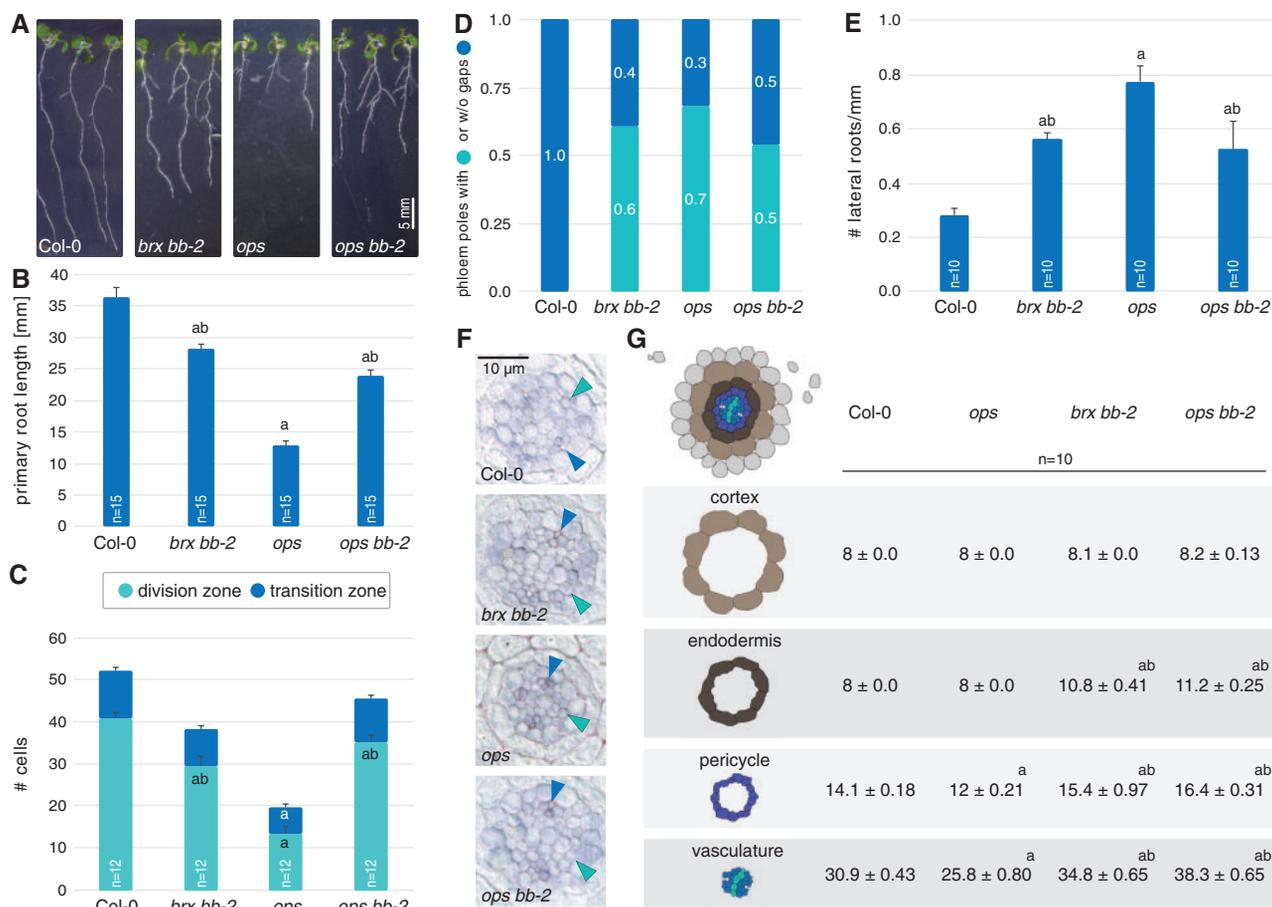
Fig. 5 Second site mutation in *BB* partially suppresses *ops* phenotypes. (A) Representative seedlings of the indicated genotypes at 7 d after germination (dag). (B) Average primary root length of the indicated genotypes at 7 dag. (C) Quantification of cortex cell number in the division zone and transition zone of 7-day-old seedlings of the indicated genotypes. (D) Quantification of gap cell frequency in the indicated genotypes at 5 dag. Differences between Col-0 and all other genotypes were statistically significant ($P < 0.001$, Fisher's exact test), but not between *bb-2 brx*, *ops* and *bb-2 ops*. (E) Lateral root density in the indicated genotypes at 12 dag. (F) Representative histological cross-sections of 6-day-old roots of the indicated genotypes, taken at the position where protoxylem (green arrowheads) has differentiated (blue arrowheads: protophloem). (G) Quantification of cell file number in roots of the indicated genotypes at 6 dag. Differences as compared with the Col-0 wild-type background (a) or *ops* mutant background (b) are statistically significant as indicated (Student's *t*-test; $P < 0.05$; mean ± SEM).

meristem and uncouple root meristematic activity from cell differentiation and elongation. It will be interesting to investigate whether mutations in *BB* homologs have a similar effect in other species, or whether such mutations could be exploited to boost root growth generically, for instance in crops.

Materials and Methods

Plant materials, growth conditions and physiological assays

Plant tissue culture, plant transformation and common molecular biology procedures such as genomic DNA isolation, plant transformation, genotyping, (whole-genome) sequencing and peptide treatments were performed according to standard procedures as previously described (Kang and Hardtke 2016, Kang et al. 2017). For plant tissue culture, seeds were surface-sterilized, germinated and grown vertically on half-strength Murashige and Skoog (MS) agar medium with or without 0.3% sucrose under continuous light of approximately 120 µE intensity at 22°C. All mutants were in the Arabidopsis Col-0 wild-type background, i.e. the described *brx-2*, *ops-2* and *bb-2* alleles (Disch et al. 2006, Rodrigues et al. 2009, Truernit et al. 2012), as well as the newly isolated bb^{P235L} allele. To produce *BB::GUS* plants, the *BB* promoter (At3g63530) was amplified using oligonucleotides 5′-GGG GAC AAG TTT GTA CAA AAA AGC AGG CTT CGA AGA AGA AGA CGG AGA AGG-3′ and 5′-GGG GAC CAC TTT GTA CAA GAA AGC TGG GTT TTC AGC TAC TGC AAT CGA GA-3′ (note: including the attB1 and attB2 sites, respectively, for GATEWAY cloning), and cloned into the pMDC163 vector. Arabidopsis Col-0 and *brx-2* plants were transformed with the construct and lines with single insertions were selected in the T_2 generation. Homozygous plants for analysis were obtained in the T_3 generation. All quantitative data shown are from single, representative replicate experiments, with genotypes assayed in parallel.

Probe unloading measurements

To measure phloem translocation rate, CFDA stock solution (10 mg ml^{-1} in dimethylsulfoxide) was diluted 1 : 100 (v/v) in ddH$_2$O and 1 µl was applied to wounded cotyledons at 4 d post-germination. Transport along sieve tubes was monitored after 45 min. using an epifluorescence microscope with a green fluorescent protein (GFP) filter. Seedlings were then mounted in propidium

iodide and imaged by confocal laser scanning microscopy (Zeiss LSM700) using a GFP filter.

Probe translocation speed assay

Arabidopsis plants were grown for 4 d, the plates were scanned, root lengths were measured using ImageJ software, and seedlings were subsequently used for CFDA loading. Plants were mounted in a plastic chamber, below a slice of solid 0.7% medium enriched with propidium iodide. CFDA was applied as described above, and the protophloem unloading zone was subsequently imaged by confocal laser scanning microscopy (Zeiss 880). Probe translocation speed was calculated by dividing the root length by the time it took CFDA to reach the root meristem unloading zone.

Division–elongation switch point calculation

Arabidopsis seedlings were grown for 5, 7, 9 and 12 d after germination. Samples were mounted in propidium iodide, and root meristems were imaged by confocal laser scanning microscopy. Cumulative cortex cell length (starting from the first cell after the ground tissue initial formative division) was measured using ImageJ software. Ten roots were used for each line to calculate the average. The linear function representing the division zone was calculated by considering the second to 20th cells (except for *brx* at 5 d after germination, where the second and 10th cells were used because the meristem was still too small). The linear function representing the elongation phase was calculated considering the third from last and last cells. The two functions were then used to calculate the intersection point, i.e. the cortex cell where the switch between division and elongation phase occurs. Details are displayed in Supplementary Fig. S1C.

Supplementary data

Supplementary data are available at PCP online.

Funding

Acknowledgments

We would like to thank Dr. Y.-H. Kang for initiation of the project, Dr. M. Lenhard for *bb-2* mutant seeds, and the Genomic Technologies Facility of the University of Lausanne for support in whole-genome sequencing.

Disclosures

The authors have no conflicts of interest to declare.

References

Beemster, G.T. and Baskin, T.I. (1998) Analysis of cell division and elongation underlying the developmental acceleration of root growth in Arabidopsis thaliana. *Plant Physiol.* 116: 1515–1526.

Beemster, G.T., De Vusser, K., De Tavernier, E., De Bock, K. and Inze, D. (2002) Variation in growth rate between Arabidopsis ecotypes is correlated with cell division and A-type cyclin-dependent kinase activity. *Plant Physiol.* 129: 854–864.

Beuchat, J., Scacchi, E., Tarkowska, D., Ragni, L., Strnad, M. and Hardtke, C.S. (2010) BRX promotes Arabidopsis shoot growth. *New Phytol.* 188: 23–29.

Breuninger, H. and Lenhard, M. (2010) Control of tissue and organ growth in plants. *Curr. Top. Dev. Biol.* 91: 185–220.

De Rybel, B., Moller, B., Yoshida, S., Grabowicz, I., Barbier de Reuille, P., Boeren, S., et al. (2013) A bHLH complex controls embryonic vascular tissue establishment and indeterminate growth in Arabidopsis. *Dev. Cell* 24: 426–437.

Depuydt, S. and Hardtke, C.S. (2011) Hormone signalling crosstalk in plant growth regulation. *Curr. Biol.* 21: R365–R373.

Depuydt, S., Rodriguez-Villalon, A., Santuari, L., Wyser-Rmili, C., Ragni, L. and Hardtke, C.S. (2013) Suppression of Arabidopsis protophloem differentiation and root meristem growth by CLE45 requires the receptor-like kinase BAM3. *Proc. Natl. Acad. Sci. USA* 110: 7074–7079.

Disch, S., Anastasiou, E., Sharma, V.K., Laux, T., Fletcher, J.C. and Lenhard, M. (2006) The E3 ubiquitin ligase BIG BROTHER controls arabidopsis organ size in a dosage-dependent manner. *Curr. Biol.* 16: 272–279.

Dong, H., Dumenil, J., Lu, F.H., Na, L., Vanhaeren, H., Naumann, C., et al. (2017) Ubiquitylation activates a peptidase that promotes cleavage and destabilization of its activating E3 ligases and diverse growth regulatory proteins to limit cell proliferation in Arabidopsis. *Genes Dev.* 31: 197–208.

Du, L., Li, N., Chen, L., Xu, Y., Li, Y., Zhang, Y., et al. (2014) The ubiquitin receptor DA1 regulates seed and organ size by modulating the stability of the ubiquitin-specific protease UBP15/SOD2 in Arabidopsis. *Plant Cell* 26: 665–677.

Gonzalez, N. and Inze, D. (2015) Molecular systems governing leaf growth: from genes to networks. *J. Exp. Bot.* 66: 1045–1054.

Gujas, B., Alonso-Blanco, C. and Hardtke, C.S. (2012) Natural Arabidopsis brx loss-of-function alleles confer root adaptation to acidic soil. *Curr. Biol.* 22: 1962–1968.

Hu, Y., Xie, Q. and Chua, N.H. (2003) The Arabidopsis auxin-inducible gene ARGOS controls lateral organ size. *Plant Cell* 15: 1951–1961.

Kang, Y.H., Breda, A. and Hardtke, C.S. (2017) Brassinosteroid signaling directs formative cell divisions and protophloem differentiation in Arabidopsis root meristems. *Development* 144: 272–280.

Kang, Y.H. and Hardtke, C.S. (2016) Arabidopsis MAKR5 is a positive effector of BAM3-dependent CLE45 signaling. *EMBO Rep.* 17: 1145–1154.

Kosarev, P., Mayer, K.F. and Hardtke, C.S. (2002) Evaluation and classification of RING-finger domains encoded by the Arabidopsis genome. *Genome Biol.* 3: RESEARCH0016.

Krizek, B.A. (1999) Ectopic expression of AINTEGUMENTA in Arabidopsis plants results in increased growth of floral organs. *Dev. Genet.* 25: 224–236.

Li, Y., Zheng, L., Corke, F., Smith, C. and Bevan, M.W. (2008) Control of final seed and organ size by the DA1 gene family in Arabidopsis thaliana. *Genes Dev.* 22: 1331–1336.

Mahonen, A.P., ten Tusscher, K., Siligato, R., Smetana, O., Diaz-Trivino, S., Salojarvi, J., et al. (2014) PLETHORA gradient formation mechanism separates auxin responses. *Nature* 515: 125–129.

Mizukami, Y. and Fischer, R.L. (2000) Plant organ size control: AINTEGUMENTA regulates growth and cell numbers during organogenesis. *Proc. Natl. Acad. Sci. USA* 97: 942–947.

Moubayidin, L., Perilli, S., Dello Ioio, R., Di Mambro, R., Costantino, P. and Sabatini, S. (2010) The rate of cell differentiation controls the Arabidopsis root meristem growth phase. *Curr. Biol.* 20: 1138–1143.

Mouchel, C.F., Briggs, G.C. and Hardtke, C.S. (2004) Natural genetic variation in Arabidopsis identifies BREVIS RADIX, a novel regulator of cell proliferation and elongation in the root. *Genes Dev.* 18: 700–714.

Mouchel, C.F., Osmont, K.S. and Hardtke, C.S. (2006) BRX mediates feedback between brassinosteroid levels and auxin signalling in root growth. *Nature* 443: 458–461.

Peng, Y., Ma, W., Chen, L., Yang, L., Li, S., Zhao, H., et al. (2013) Control of root meristem size by DA1-RELATED PROTEIN2 in Arabidopsis. *Plant Physiol.* 161: 1542–1556.

Perilli, S., Di Mambro, R. and Sabatini, S. (2012) Growth and development of the root apical meristem. *Curr. Opin. Plant Biol.* 15: 17–23.

Rodrigues, A., Santiago, J., Rubio, S., Saez, A., Osmont, K.S., Gadea, J., et al. (2009) The short-rooted phenotype of the brevis radix mutant partly reflects root abscisic acid hypersensitivity. *Plant Physiol.* 149: 1917–1928.

Rodriguez-Villalon, A., Gujas, B., Kang, Y.H., Breda, A.S., Cattaneo, P., Depuydt, S., et al. (2014) Molecular genetic framework for protophloem formation. *Proc. Natl. Acad. Sci. USA* 111: 11551–11556.

Rodriguez-Villalon, A., Gujas, B., van Wijk, R., Munnik, T. and Hardtke, C.S. (2015) Primary root protophloem differentiation requires balanced phosphatidylinositol-4,5-biphosphate levels and systemically affects root branching. *Development* 142: 1437–1446.

Santuari, L., Sanchez-Perez, G.F., Luijten, M., Rutjens, B., Terpstra, I., Berke, L., et al. (2016) The PLETHORA gene regulatory network guides growth and cell differentiation in Arabidopsis roots. *Plant Cell* 28: 2937–2951.

Santuari, L., Scacchi, E., Rodriguez-Villalon, A., Salinas, P., Dohmann, E.M., Brunoud, G., et al. (2011) Positional information by differential endocytosis splits auxin response to drive Arabidopsis root meristem growth. *Curr. Biol.* 21: 1918–1923.

Scacchi, E., Salinas, P., Gujas, B., Santuari, L., Krogan, N., Ragni, L., et al. (2010) Spatio-temporal sequence of cross-regulatory events in root meristem growth. *Proc. Natl. Acad. Sci. USA* 107: 22734–22739.

Truernit, E., Bauby, H., Belcram, K., Barthelemy, J. and Palauqui, J.C. (2012) OCTOPUS, a polarly localised membrane-associated protein, regulates phloem differentiation entry in Arabidopsis thaliana. *Development* 139: 1306–1315.

Vanhaeren, H., Nam, Y.J., De Milde, L., Chae, E., Storme, V., Weigel, D., et al. (2017) Forever young: the role of ubiquitin receptor DA1 and E3 ligase BIG BROTHER in controlling leaf growth and development. *Plant Physiol.* 173: 1269–1282.

Xia, T., Li, N., Dumenil, J., Li, J., Kamenski, A., Bevan, M.W., et al. (2013) The ubiquitin receptor DA1 interacts with the E3 ubiquitin ligase DA2 to regulate seed and organ size in Arabidopsis. *Plant Cell* 25: 3347–3359.